Quantifying the Carbon Storage in Urban Trees Using Multispectral ALS Data

Xinqu Chen, Chengming YE, Jonathan Li, *Senior Member, IEEE*, and Michael A. Chapman

***Abstract*—This paper presents a new method for quantifying the carbon storage in urban trees using multispectral airborne laser scanning (ALS) data. This method takes the full advantage of multispectral ALS range and intensity data and shows the feasibility of quantifies the carbon storage in urban trees. Our method consists of four steps: multispectral ALS data processing, vegetation isolation, dendrometric parameters estimation, and carbon storage modeling. Our results suggest that ALS-based dendrometric parameter estimation and allometric models can yield consistent performance and accurate estimation. Citywide carbon storage estimation is derived in this paper for the Town of Whitchurch–Stouffville, Ontario, Canada, by extrapolating the values within the study area to the entire city based on the specific proportion of each land cover type. The proposed method reveals the potential of multispectral ALS data in land cover mapping and carbon storage estimation at individual-tree level.**

***Index Terms*—Airborne laser scanning (ALS), allometric models, carbon storage, diameter at breast height (DBH), multispectral.**

I. Introduction

With the continuing growth of the global population, urbanization has become an inevitable trend. Today, over 50% of the global population resides in cities, and by 2050, urban areas will hold up to another 2.5 billion people, equivalent to 66% of the global population. Intensive urban developments and economic activities increase the energy consumption and result in greenhouse gas emissions [1]–[3]. As urban land covers expand, direct losses of vegetation cover also occur. Without vegetation covers acting as the largest carbon sink, deforestation becomes the second largest contributor to greenhouse gases [4].

Urban vegetation has drawn the direct attention of city planners and policy makers, considering the importance of trees in urban climate modification and energy conservation. In the context of Canada's climate, annual cooling energy use can be reduced 10%–19% by planting vegetation proximate to the houses and increasing the albedo of urban surfaces [5], [6]. Citywide urban trees reduce air pollution through direct dry deposition and also influence the cooling of the ambient temperature, which slows smog formation. Vegetation contributes the largest proportion of carbon storage, which in return reduces the rate of climate warming and urban heat islands [7]. Urban trees both sequester CO_2 and store excess carbon in biomass (71% of the total urban carbon storage), which significantly influences the environmental quality and human health [8], [9]. Preserving carbon storage and improving green space infrastructure in urban areas has significant environmental benefits [10]. Consequently, estimation and monitoring of urban carbon stocks and green space become important indeed. In literature, the carbon content stored in individual trees can be assessed through aboveground dry-weight biomass calculation using allometric equations. Dendrometric parameters, such as individual tree height or crown diameters, are generally used in the allometric equations to derive diameter at breast height (DBH). Dry biomass is then calculated using the allometric model, with DBH as the input, and further transformed to carbon storage with a conversion rate of around 0.5 [11], [12].

Previous studies have successfully extracted detailed vegetation covers from very high-resolution multispectral imagery, such as QuickBird, and applied it to the canopy height model (CHM) derived by airborne laser scanning (ALS) data for dendrometric measurements and biomass estimation in both forestry and urban studies [13]–[17] estimated carbon storage in urban trees for the city of Boston by developing an ALS-height-only regression model to estimate the carbon storage across the city. A total of 404 accurately segmented tree crowns from the normalized DSM (nDSM) were split into 284 samples for model fitting and 120 samples for validation. The reason for using a simple linear regression of tree biomass and height was to avoid the influence of crown segmentation results. A R^2 of 0.79 was found between field-estimated biomass and model-predicted biomass. Schreyer *et al.* estimated the carbon storage in urban trees, and its distribution was extrapolated to the entire city of Berlin in terms of land use types [14]. This study did not propose a region-specific allometric model for the study area, but applied the ALS-DBH model developed and a carbon allometric model using DBH as the only independent variable. Eighty-seven percent of the modeled DBH showed an underestimation, which was further calibrated by a weighted arithmetic average DBH. The carbon storage in urban trees was calculated

Manuscript received February 26, 2017; revised February 1, 2018, May 14, 2018, and June 28, 2018; accepted July 17, 2018. This work was supported in part by the National Key Technologies Research and Development Program of China (2016YFB0502600) and in part by the Key Program of Sichuan Bureau of Science and Technology (2018ZDYF1214). *(Corresponding author: Chengming YE.)*

X. Chen and J. Li are with the Department of Geography and Environmental Management, University of Waterloo, Waterloo, ON N2L 3G1, Canada (e-mail: x383chen@uwaterloo.ca; junli@uwaterloo.ca).

C. YE is with the Key Laboratory of Earth Exploration and Information Technology of Ministry of Education, Chengdu University of Technology, Chengdu 610059, China (e-mail: rsgis@sina.com).

M. A. Chapman is with the Department of Civil Engineering, Ryerson University, Toronto, ON M5B 2K3, Canada (e-mail: mchapman@ryerson.ca).

Color versions of one or more of the figures in this paper are available online at http://ieeexplore.ieee.org.

Digital Object Identifier 10.1109/JSTARS.2018.2859957

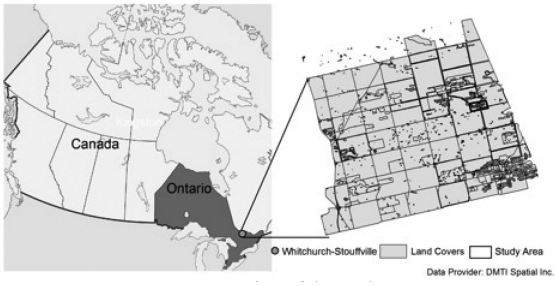

Fig. 1. Location of the study area.

as half of the model-based biomass, regardless of the genus. Meanwhile, the crown base height was assumed to be half of the ALS-derived height, and the crown width was calculated in 16 directions with a series of criteria, instead of the conventional estimation of crown width in four directions as proposed in [18] or as used in [19].

With the emerging multispectral LiDAR technology, it became possible to obtain both the range and multiple reflectance data from a single data source. The first commercial multispectral ALS system, Titan, released by Teledyne Optech, Inc., has integrated three laser channels at wavelengths of 532, 1064, and 1550 nm, respectively. These three channels produce independent scan lines by sending pulses with separate forward angles (the NIR channel has a 0° forward angle; the SWIR channel has a 3.5° forward angle; and the green channel has a 7.0° forward angle). This emerging ALS system showed great potential in land cover mapping without the aid of passive multispectral images [20], [21]. This active laser system can largely avoid those factors commonly associated with passive optical sensors, such as weather conditions and shadow effects. However, the potential of ALS intensity currently remains undervalued, and the applications of this newly released system are at an early stage of development.

Given the current state of development of tree inventory with typical ALS data, this paper aims to explore the feasibility of multispectral ALS range and intensity data in carbon storage estimation. To achieve this, vegetation covers are first classified based on multispectral ALS range and intensity data by applying a support vector machine (SVM) classifier. Second, dendrometric parameters, such as tree height and crown diameter, are derived, in order to establish an allometric relationship between ALS-derived measurements (tree height and crown diameter) and the field-measured parameter (DBH) through regression modeling. Finally, this study quantifies the carbon storage in urban trees for the Town of Whitchurch-Stouffville, Ontario, Canada.

II. Study Area and Data Sources

The study area is located in the Town of Whitchurch-Stouffville, Ontario, Canada, which is a municipality in the Greater Toronto Area (see Fig. 1). The study area is characterized by a typical residential landscape. It contains two water bodies (Musselman Lake and Winsor Lake) and three land cover types: residential area, open area (grassland and woody area), and park and recreation [22]. The residential area consists of single detached dwellings with mature street and backyard trees planted at least ten years ago [23]. There are different types of trees that live in the study area, including deciduous trees, such as maple, ash, oak, elm, black cherry, basswood, and conifers [24].

Two multispectral ALS datasets were acquired by the Teledyne Optech Titan system on July 2, 2015. The datasets had two flight lines that covered and intersected at the study area. The flight altitudes were above 1000 m with a pulse frequency of 100 kHz for each channel, yielding an average point spacing of 0.8 m per point and an average point density of 7.7 point/m². The three laser channels are 532, 1064, and 1550 nm.

Field data were collected on February 9, 2016. A total of 40 trees were sampled in the field that contained four attributes; height, DBH, crown diameter, and biomass were recorded for every single tree. Tree heights were measured using a hypsometer in units of the meter. DBH was measured with a diameter tape in units of the centimeter. Since the field measurement was conducted during the leaf-off season, the third attribute, crown diameter, was measured using high-resolution Google Earth images. The crown diameter is defined as the mean of the maximum crown diameter and the diameter measured at the direction perpendicular to the maximum, using the Ruler tool in Google Earth in units of the meter. The fourth attribute, single tree carbon storage, is estimated by plugging the field-measured DBH and tree height into the Canadian national aboveground all-species biomass equations [25]. The equations calculate the dry aboveground biomass by relating tree height and DBH to each biomass component, such as wood, bark, and foliage, with a uniform relationship $\mathrm{Biomass} = \beta_1 \mathrm{DBH}^{\beta_2} H^{\beta_3}$; where β_1, β_2, and β_3 are the parameters generated for the all-species group with different values according to the tree compartments. The carbon storage in sampled trees was then defined as half of the sum of the dry aboveground biomass in each compartment.

III. Method

Our method consists of four parts: ALS data processing, vegetation isolation, dendrometric parameter extraction, and carbon storage modeling (see Fig. 2).

A. ALS Data Processing

After removing outliers and rectifying the ALS intensity values, point clouds from two flight strips were merged together; in total, three ALS point clouds were acquired by the Titan laser channels. Then, each point cloud was rasterized into an intensity image with a ground resolution of 1 m. The pixel size was selected according to the point spacing of the dataset. By selecting the pixel size close to the point spacing, most of the pixels can contain at least one point, and the vertical distribution of the points can be largely highlighted. In this way, points were grouped into 1-m grids and the pixel values were assigned by the mean intensity of the points within the grid. For the grids which had no point filled in, the grid values were interpolated linearly by searching the neighbors. Here, three mean intensity

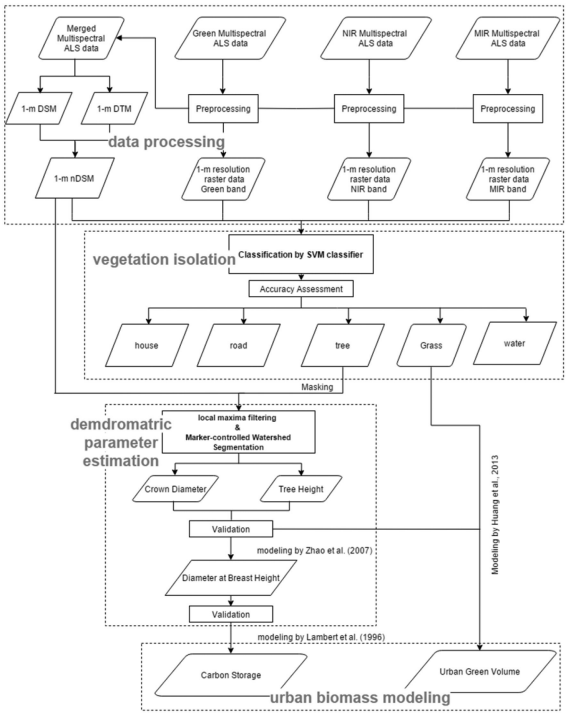

Fig. 2. Workflow of the proposed method.

raster data were generated for channels 532, 1064, and 1550 nm, respectively.

Besides the generation of ALS intensity images, DSM and DTM were created from the raw ALS by a ground-point filtering and rasterization process. The whole ALS dataset was then classified into ground and nonground classes. DTM raster data were generated by rasterizing all the ground points into 1-m grids, based on the linear interpolation method. The DSM was generated in a similar way by using the nonground class, and the maximum height within the grid was assigned to the pixel values. In this way, the points that represented the treetops could be largely reserved. Finally, nDSM raster data were acquired by subtracting the DTM from the DSM.

B. Vegetation Isolation

Besides the multispectral intensity and nDSM data described above, two additional indices were derived as follows:

$$\mathrm{pNDWI} = \frac{C_{\mathrm{Green}} - C_{\mathrm{NIR}}}{C_{\mathrm{Green}} + C_{\mathrm{NIR}}} \tag{1}$$

$$\mathrm{pNDVI} = \frac{C_{\mathrm{NIR}} - C_{\mathrm{SWIR}}}{C_{\mathrm{NIR}} + C_{\mathrm{SWIR}}} \tag{2}$$

where C_{Green}, C_{NIR}, and C_{SWIR} refer to the laser channels at 532, 1064, and 1550 nm, respectively.

By visually examining the pNDWI and pNDVI indices (see Fig. 3), both the pNDVI and pNDWI showed good discrimination for artificial objects. These two indices can facilitate the manual selection of training samples and work as the ancillary data in the classification process. The contribution of these two indices to the overall classification accuracy was analyzed. A total of six input data, including 1) Green channel intensity, 2) NIR channel intensity, 3) SWIR channel intensity, 4) nDSM, 5) pNDWI, and 6) pNDVI, were generated and input into the classification scheme.

(a) (b)

Fig. 3. Examples of ALS-intensity-derived indices.

Because the study area was characterized by a simple residential landscape, it could be grouped into six land cover types, including water, house, road, grass, tree, and open area. However, due to the bathymetry capability of the channel at 532 nm, water points in the study area tended to have an irregular intensity that was induced by the interaction of laser points with both the water surface and organic matter underneath. Hence, water bodies, including Musselman Lake, Windsor Lake, and one small water region, were masked out of the dataset, resulting in only five land cover types being trained and classified in this study. Interpreting land cover types from ALS intensity was not as easy as from passive optical images. Certain land cover types, such as grass and open area, could be distinguished from only one or two intensity data and could hardly be identified from the rest.

A SVM classifier was selected to perform land cover classification with multispectral ALS-derived data due to the popularity of SVM in typical ALS-related classification studies, making the classification result of this study comparable to previous studies. The SVM classification was performed on three combinations of the input data. The selection of input data was mainly designed for showing the benefits of multispectral ALS in land cover classification $(\mathrm{Greeen} + \mathrm{NIR} + \mathrm{SWIR} + \mathrm{nDSM} + \mathrm{pNDWI} + \mathrm{pNDVI})$, compared with typical LiDAR data $(\mathrm{Gree} + \mathrm{NIR} + \mathrm{SWIR} + \mathrm{NDSM})$. Meanwhile, $\mathrm{Selection1}(\mathrm{NIR} + \mathrm{nDSM})$ was designed to examine the contribution of multispectral-intensity-derived indices in overall classification accuracy.

C. Dendrometric Parameter Estimation

The tree-isolated nDSM was also referred to as the CHM, a model displaying tree positions by tree crowns in a top-down view and storing the height values in pixels. A 3×3 local maxima filter was first employed on the CHM to detect treetops. A pixel with the highest value amongst its eight neighbors was defined as the treetop. To eliminate the commission errors associated with the local maxima filtering and detect the true treetop pixels, the local maxima in the CHM was further filtered by the ALS intensity data. The ALS intensity values were dependent not only on the reflectivity of the object, but also on the range between the sensor and the object. A true treetop pixel

would have both high intensity and height values. Under this assumption, another 1-m raster data were generated as the sum of the maximum intensity of the first return in each channel. The clusters of local maxima in the CHM which had more than 15 pixels together were further extracted, and only the pixels that were also the local maxima in the maximum intensity layer were retained in the final treetop results. Previous studies relied on changing the window size and shape of the filter to refine the treetops [26], [27]. These approaches were not suitable here because the CHM resolution (1 m) generated in this study was relatively coarse so that increasing the window size of the local maxima filter would result in excluding small tree crowns.

The Marker-controlled watershed segmentation was applied to segment the CHM into individual tree crowns by defining the predetected treetops as the markers. In this way, every predetected treetop would have one closed segment. The performance of the segmentation in isolating tree crowns was evaluated by the absolute accuracy, calculated as

$$\text{absolute accuracy}_{\text{tree isolation}} = \frac{n_{1,1}}{n_{\text{total}}} \tag{3}$$

where $n_{1,1}$ is the number of detected crown segments which have a one-to-one relationship to the ground truth and n_{total} is the number of tree crowns in the ground truth. Tree height is defined as the average of the local maxima within each segment, and crown diameter is defined as the average of the maximum crown diameter passing through the center of the local maxima and the one measured at the perpendicular direction.

To evaluate the accuracy of the ALS-derived dendrometric parameters, the ALS-derived tree height and crown diameter were compared with the field measurements. The crown segments generated from the ALS data were matched with the 40 field-sampled trees, and the RMSE and bias were calculated to compare the ALS-derived dendrometric parameters with field samples

$$\text{Bias} = \frac{\sum_{i=1}^{n} X_{\text{ALS},i} - X_{\text{field},i}}{n} \tag{4}$$

$$\text{RMSE} = \sqrt{\frac{\sum_{i=1}^{n} X_{\text{ALS},i} - X_{\text{field},i})^2}{n}} \tag{5}$$

$$\text{RMSE}\% = \frac{\text{RMSE}}{\bar{X}_{\text{ALS}}} \tag{6}$$

where n is the number of field samples, which equaled 40 trees in this study; X refers to the values of dendrometric parameters (height or crown diameter) measured either in the field or from the ALS data; and $\bar{X}_{\text{ALS}}$ is the arithmetic mean of the ALS-derived measurements. Moreover, a linear regression model was fit to the ALS-derived tree height and crown diameter to determine if there was a strong correlation between these two variables

D. Carbon Storage Modeling

In order to predict the carbon storage in trees, a multiple linear regression model was developed empirically to fit the data, with the ALS-derived dendrometric parameters as the independent predictors and the field-measured DBH as the predicted variable. The empirical equation derived from the ALS-DBH linear regression model has the form

$$\text{DBH}_{\text{Field}} = a \cdot CD_{\text{ALS}} + b \cdot H_{\text{ALS}} + c. \tag{7}$$

The 40 field-sampled trees were split into two datasets, with 20 trees used for model parameterization and the remaining 20 trees reserved for validation. To eliminate the influence of tree locations in model fitting, each ten adjacent tree samples were grouped together under one sampling location, resulting in a total of four sampling groups. Six combinations of training and validation datasets were chosen by selecting two sampling locations out of four for model development and using the remaining two locations for validation. All six models were developed at a 0.05 significance level and were fitted through a cross-validation process. The parameters generated for each model were collected. The predictive power of the regression models and the performance were inspected by the coefficient of determination (R^2), and the accuracy of the prediction was examined by the RMSE of the predicted parameters. Comparing R^2 and RMSE of the six ALS-DBH regression models, the one with high R^2 in the model fitting and low RMSE in the validation was selected to predict DBH.

After selecting the ALS-DBH regression model, the ALS-estimated DBH and height were plugged into the Canadian national aboveground biomass equations proposed in [25] to estimate the carbon storage in trees. As reported in [25], the set of equations based on DBH and height for all species was selected to calculate the biomass, since no genus or species information was available in this study. The aboveground biomass was estimated as the sum of biomass in tree compartments (foliage, branch, wood, and bark) [23]. The carbon stored in trees was estimated as the half of total biomass. The carbon storage predicted by the ALS-derived parameters was compared with that estimated by the field-measured DBH and height and evaluated by the RMSE and R^2.

To show whether carbon storage in trees varied with land cover types, the ALS-derived tree-crown segments were first converted into vector data in GIS, with the amount of carbon storage stored in the attributes. The carbon storage within each land cover type was calculated by adding up all the carbon storage in trees and dividing by the area of the land cover type. For the Town of Whitchurch-Stouffville, the carbon stocks were extrapolated by multiplying the specific carbon amount per unit area with the total area of each land cover type. For those land cover types which were excluded in the study area (namely government and institutional areas and industrial sites), the carbon stored in government and institutional areas were given the same amount per unit area as the residential, but the carbon stored in industrial sites was given zero. Then, a citywide carbon storage map was created.

IV. Results and Discussion

A. Analysis of ALS Data for Land Cover Classification

The classification at tree genus or species level is important, especially for precise biomass estimation, the spectral patterns of the tree class were examined further to find if current

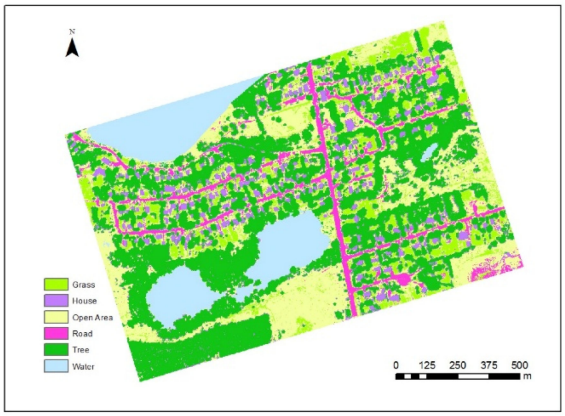

Fig. 4. Land covers of the study area.

TABLE I
ACCURACY REPORT FOR CLASSIFICATION RESULTS

Method	Green	NIR	SWIR	nDSM	pNDWI	pNDVI	OA(%)
Selection 1	√	√	√	√	√	√	90.23
Selection 2	√	√	√	√	×	×	89.12
Selection 3	×	√	×	√	×	×	79.04

multispectral LiDAR datasets could distinguish the tree class into conifer and deciduous trees. After confirming the tree types in Google Earth, there were no obvious distinctions between the tree genus by visual observations. However, through close visual observation of the pNDVI dataset, the trees with dark-color leaves, such as the Crimson King Maple tree, could stand out from the tree class. The multispectral ALS datasets generated in the study may not be sensitive enough to provide the separate classification for conifers and deciduous trees. However, the analysis presented here shows that the multispectral ALS intensity may be influenced by factors such as the color/reflectivity of the objects, which in turn will be beneficial to studies of tree mortality, rooftop solar energy, etc.

Accuracy assessment was conducted on the classification results in order to examine the classification performance of multispectral ALS data. Fig. 4 shows the final classification map. The combination of all six input data achieved the highest overall accuracy among the three selections (see Table I). The 89% overall accuracy was achieved using the ALS-derived raster data, which indicated that the contributions of the two calculated indices to the overall accuracy were not significant. The comparison between typical ALS data and multispectral ALS data on land cover classification was also conducted; the same classification process was applied to the nDSM and NIR bands only. The overall classification accuracy in the use of typical ALS data was around 79%.

B. Validation Statistics

The accuracies of ALS-derived tree height and crown width were assessed by the samples measured in the field. For the ALS-derived tree height, an RMSE of 1.21 m (relative RMSE = 6.8%) and a negative bias of 0.2 m (relative bias = −0.1%) are given in Table II. For the ALS-derived crown width, an RMSE of 1.47 m (relative RMSE = 16.4%) and a negative bias of 0.18 m (relative bias = −2%) were observed. The tree height

TABLE II
VALIDATION STATISTICS FOR ALS-DERIVED DENDROMETRIC PARAMETERS

Parameter	RMSE (m)	RMSE (%)	Bias (m)	Bias (%)
Height	1.21	6.8	- 0.20	- 0.1
Crown width	1.47	16.4	- 0.18	- 2.0

TABLE III
RESULTS OF MODEL FITTING AND MODEL VALIDATION

Model	Model Fit R^2	Model Fit RMSE (cm)	Validation R^2	Validation RMSE (cm)
1	0.83	5.35	0.80	6.82
2	0.86	6.60	0.76	5.60
3	0.86	3.86	0.71	8.25
4	0.75	7.89	0.77	4.82
5	0.78	5.59	0.85	6.55

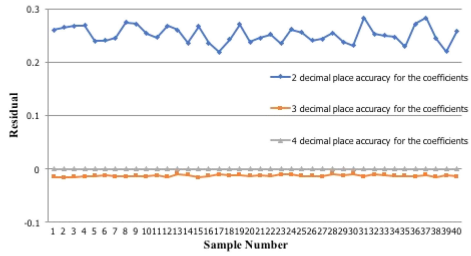

Fig. 5. Residual plots for model-predicted DBH generated by coefficients with two, three, and four decimal places.

was underestimated because of the undergrowth and factors related to the flight height (1000 m) and the point density (7 to 8 points/m^2). The relative RMSE of crown width was mainly caused by the resolution of the CHM and the results of crown segmentation.

C. Validations for ALS-DBH and Tree Carbon

The results of model fitting and validation of the six ALS-DBH regression models are listed in Table III. The 40 field-measured samples were previously split into four groups, with ten trees in each group. The models were iteratively fitted by 20 trees selected from two groups out of four and were validated by the remaining 20 trees. Model 2 was selected as the overall best model to predict DBH in this study because it has a relatively high coefficient of determination ($R^2 = 86\%$) from model fitting and a relatively low RMSE (5.6 cm) from the validation. Equation (7) is then modified as

$$\mathrm{DBH} = (-0.2958)\,CD + 3.2637\,H - 11.2792. \quad (8)$$

To determine the number of decimal places for the coefficients in the regression equation, the residuals between the DBH values predicted by the coefficients with eight decimal places and those predicted by coefficients rounded to two, three, and four decimal places, respectively, are compared in Fig. 5.

To keep high prediction accuracy, coefficients in the regression model are rounded to four decimal places. Moreover, the R^2between field-measured tree height and crown width was calculated as 0.34, indicating insignificant correlation between these two variables. Though DBH cannot be directly measured on the CHM, all the generated ALS-DBH models showed that

TABLE IV
ACCURACY OF ALS-PREDICTED VERSUS FIELD-MEASURED RESULTS

Parameter	RMSE (m)	RMSE (%)	Bias (m)	Bias (%)
DBH	6.39	13.1	0.44	0.1
Carbon	142.0	28.6	14.4	2.9

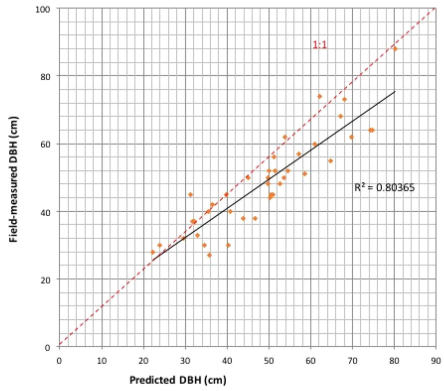

Fig. 6. Scatterplot of ALS-modeled DBH versus field-measured DBH.

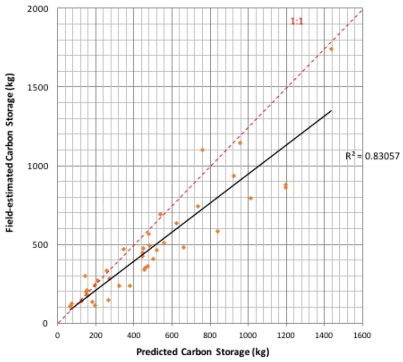

Fig. 7. Scatterplot of the ALS-predicted carbon storage versus field-estimated carbon storage.

the DBH correlated well with ALS measurements. The accuracies of the ALS-modeled DBH and ALS-derived carbon storage are given in Table IV. The predicted DBH using ALS-derived parameters corresponded to an RMSE of 6.4 cm (relative RMSE = 13.1%) and a bias of 0.4 cm. The relationship between field-measured DBH and ALS-modeled DBH is plotted in Fig. 6. The results are compared with the reference carbon storage estimated by field-measured DBH and plotted in Fig. 7. The R^2 of DBH and carbon storage was above 0.80. The predicted carbon storage using ALS-modeled DBH corresponded to an RMSE of 142 kg (28.6%) and a bias of 14.4 kg.

D. Analysis of ALS-Estimated Results

The accuracy of tree-height measurements using ALS data has previously been studied in [28]–[30]. As found in [28], as flight altitude increased from 400 to 1500 m, the accuracy of tree heights lowered from 0.76 to 1.16 m for single tree species. As reported in [29], the best methods which utilized the local maxima finding with a point density of 8 points/m^2 could obtain an RMSE of 60 to 80 cm for tree heights. As shown in [30], the bias of tree-height measurements could decrease from −1.48 to −0.72 m if the point density increased from 3.5 to 9 points/m^2. The RMSE achieved in this study is in line with these studies and is potentially affected by the errors generated during the field measurements. Both overestimations of the crown size and underestimations of the tree heights are likely a result of the overlaying crown covers of the dominant tree and the suppressed trees, but could be mitigated if the resolution of CHM is at the submeter level. The results of ALS-modeled DBH are in line with the findings in [31] and [32], regarding the tree height and crown diameter as good predictors to predict DBH using linear regression. The accuracy found in this study is higher than in these two studies. As reported in [31], an RMSE for ALS-estimated DBH of Norway spruce was 35%. A lower RMSE (4.9 cm) and higher R^2 compared to this study was reported in [32]. However, considering that in [32] the accuracies were for single tree species, which had an average DBH of 29.55 cm, and that they used all 43 sampled trees to construct the model and validate the model using the same dataset, the RMSE% and R^2 in their study would understandably be higher than that in this study [32]. For aboveground biomass, an RMSE of 47% for single tree species was reported in [30]. An RMSE of 35.1% was achieved for biomass estimation in [28]. Though the achieved accuracy of carbon estimation is higher in this study, these studies are not entirely comparable because some studies used field-destructive measurements as reference data, which were not available in this study. Also, because genus information is not available, the estimation of carbon stocks was done by the allometry equations for all species in Lambert *et al*. so that the derived carbon mainly depended on the ALS-derived DBH and height, with a little consideration given to the differences in species [25].

E. Analysis of Carbon Storage

There were a total of 2555 dominant trees in the study area. The trees were located along the roadsides, in the backyards, and around the lakes. The average tree carbon was 484.3 kg and resulted in a total of 1.24 kt C (10^3 tons carbon). The study area could be divided into four land use types: residential, park and recreational, open area, and water.

The open area occupied the largest portion of the study area, 47.0 ha. The residential area occupied 25.8 ha. The park had a small area of 2.5 ha. The extracted carbons in trees were, therefore, grouped based on the land use type, and the amount of carbon stored in each land cover type was calculated. Within the study area, the open area contained the largest tree carbon stocks (682.7 t), followed by the residential area (362.6 t), and, finally, the parks and recreational area (29.2 t). The tree carbon storage for the open area, residential area, and parks on a per-unit-area basis were 14.54, 14.08, and 11.57 t C/ha, respectively. Citywide open area occupied 83.7% (191.5 km^2) of the total city area and contained the largest carbon storage, 278.4 kt C. Residential area covered 8.3% (19.4 km^2) of the total city area and contained 27.3-kt C tree carbons. Parks covered 12.8 km^2 with a total carbon storage estimated at 14.8 kt C. Fig. 8 shows the carbon storage map of the study area, which indicates that large tree carbon stocks are accumulated in urban environments and are distributed heterogeneously among land use types.

The estimated tree carbons in the study area were in line with the estimation of carbon storage in Canadian urban trees conducted by researchers at Environment Canada [15]. As reported

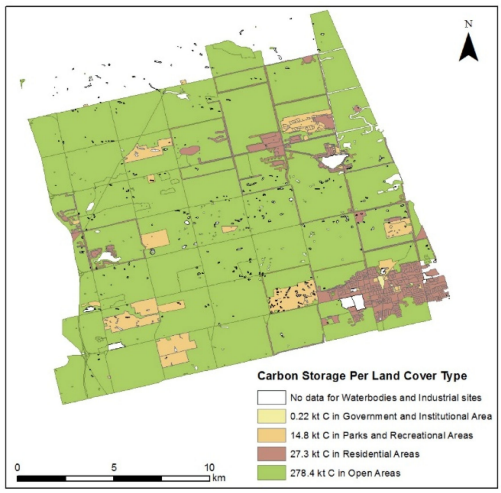

Fig. 8. Carbon storage map of the study area.

in [15], the carbon stocks in trees were estimated by applying the crown cover area of urban trees and a Canadian-specific area-based growth rate for urban trees. Also, as reported in [15], a total urban area of 5317 km² in the Mixedwood Plains (Ontario's smallest ecozone) with an estimation of carbon storage at 9177.6 kt C, resulted in a carbon storage per unit urban area as 17 kt C/ha. This is slightly more than what has been predicted in this study (around 14 kt C/ha). The main source of the difference comes from the approaches to estimate the biomass amounts between this study and that used in [15]. Our case study found that carbon storage in urban trees can be quantified effectively when multispectral ALS range and intensity data are used.

V. Conclusion

This paper proposed a workflow to map land covers and estimate aboveground carbon storage in trees at a spatial resolution of 1 m using multispectral ALS data. This paper shows that the improved classification results can be obtained solely from multispectral ALS datasets. Our results demonstrated that the overall accuracies achieved using multispectral ALS data range from 89.12% to 90.23%, which is about 11% higher than that obtained using traditional single-wavelength ALS data (with an overall accuracy of 79.04%). Spectral patterns for impervious surfaces (road, rooftops) and single-return vegetation (grass) are observed to have similar patterns in the optical imagery. The dendrometric parameters at single-tree level can be derived directly from the multispectral ALS data. It also shows how the use of both spectral and geometric properties of multispectral ALS data can improve the detection of treetops. The improvement could be more significant if the resolution of the CHM were finer.

This paper presented the feasibility of applying forest-based allometric methods to assess carbon stocks in urban environments. Dominant trees with fewer underneath or nearby trees were better detected and analyzed in the study. Though DBH cannot be directly measured from ALS data, the ALS-predicted DBH remains a power predictor for estimating tree carbon at the individual-tree level. More accurate tree carbon measurements could be obtained if genus information and crown base heights were further investigated. An improvement of the derivation of the crown width would also help in the better prediction of tree carbon stocks. This paper derived similar carbon amounts per unit area in both residential areas and open areas within the study area because the open area had twice the size of the residential area but the density of the canopy covers was less than it was in the residential area. Citywide carbon storage estimation was derived in this paper by extrapolating the values within the study area to the entire city, based on the specific proportion of each land cover type in the city. This approach is applicable here because the Town of Whitchurch-Stouffville has a relatively simple city structure, the study area has included the major components of the city, and those land covers excluded in the study area only occupied a small proportion of the entire city.

Urban ecosystems are an important component in the global carbon cycle. In the context of urban sprawl, quantifying the carbon storage for urban areas is very important in terms of getting reliable estimations of carbon sequestration rate and magnitude, but it is a difficult and complex task that requires advanced analysis techniques and data sources to achieve fine-scale estimation. The methods developed here provide an accurate and detailed estimate of how urban trees in a Canadian city play the role of a carbon sink. The presented approach of estimating carbon stocks in urban trees takes advantage of the available Canada-wide allometry relationship between biomass and tree DBH and height, as well as the power of the ALS system in providing the estimation of dendrometric parameters. The methodology proposed does not require destructive sampling or large-scale field works. It is applicable to other urban areas and is beneficial to the better understanding of urban carbon budgets and urban heat island effects. It also provides valuable information on the impact of climate change on city planners.

In conclusion, this paper has developed a detailed workflow to estimate tree carbon stocks from multispectral ALS data by using a series of techniques including SVM classification, watershed segmentation, and allometry-based linear regression modeling. This paper also demonstrated the strong capability of multispectral ALS data in land cover mapping and tree-level inventory in urban environments. The experimental results also indicate that our method is very promising for quantifying the carbon storage in urban trees when taking full advantage of multispectral ALS range and intensity data.

References

[1] J. G. Cartera, J. Handleya, T. Butlinb, and S. Gill, "Adapting cities to climate change—Exploring the flood risk management role of green infrastructure landscapes," *J. Environ. Plan. Manage.*, vol. 61, pp. 1535–1552, Sep. 2017, doi: 10.1080/09640568.2017.1355777.

[2] W. Lutz, "How population growth relates to climate change," *Proc. Nat. Acad. Sci.*, vol. 114, no. 46, pp. 12103–12105, Nov. 2017.

[3] D. Dodman, J. Bicknell, and D. Satterthwaite, Eds., *Adapting Cities to Climate Change: Understanding and Addressing the Development Challenges*. New York, NY, USA: Routledge, 2012.

[4] T. Johnson, Deforestation and greenhouse-gas emissions, Council on Foreign Relations, 2009.

[5] T. Xu, J. Sathaye, H. Akbari, V. Garg, and S. Tetali, "Quantifying the direct benefits of cool roofs in an urban setting: Reduced cooling energy use and lowered greenhouse gas emissions," *Build. Environ.*, vol. 48, pp. 1–6, 2012.

[6] M. Sawka, A. A. Millward, J. Mckay, and M. Sarkovich, "Growing summer energy conservation through residential tree planting," *Landscape Urban Plan.*, vol. 113, pp. 1–9, 2013.
[7] Z. G. Davies, J. L. Edmondson, A. Heinemeyer, J. R. Leake, and K. J. Gaston, "Mapping an urban ecosystem service: quantifying above-ground carbon storage at a city-wide scale," *J. Appl. Ecol.*, vol. 48, no. 5, pp. 1125–1134, 2011.
[8] G. H. Donovan and D. T. Butry, "Trees in the city: Valuing street trees in Portland, Oregon," *Landscape Urban Plan.*, vol. 94, no. 2, pp. 77–83, 2010.
[9] S. Roy, J. Byrne, and C. Pickering, "A systematic quantitative review of urban tree benefits, costs, and assessment methods across cities in different climatic zones," *Urban Forestry Urban Greening*, vol. 11, no. 4, pp. 351–363, 2012.
[10] M. van den Berg, W. Wendel-Vos, M. van Poppel, H. Kemper, W. van Mechelen, and J. Maas, "Health benefits of green spaces in the living environment: A systematic review of epidemiological studies," *Urban Forestry Urban Greening*, vol. 14, no. 4, pp. 806–816, 2015.
[11] H. Lieth, "The role of vegetation in the carbon dioxide content of the atmosphere," *J. Geophy. Res.*, vol. 68, no. 13, pp. 3887–3898, 1963.
[12] R. H. Whittaker and G. E. Likens, "Carbon in the biota," in *Carbon and the Biosphere*, G. M. Woodell and E. V. Pecans, Eds. Washington, DC, USA: Technical Information Center, U.S. Atomic Energy Commission, 1973, pp. 281–302.
[13] Y. Huang *et al.*, "Toward automatic estimation of urban green volume using airborne LiDAR data and high resolution remote sensing images," *Front. Earth Sci.*, vol. 7, no. 1, pp. 43–54, 2013.
[14] J. Schreyer, J. Tigges, T. Lakes, and G. Churkina, "Using airborne LiDAR and QuickBird data for modelling urban tree carbon storage and its distribution—A case study of Berlin," *Remote Sens.*, vol. 6, no. 11, pp. 10636–10655, 2014.
[15] J. Pasher, M. McGovern, M. Khoury, and J. Duffe, "Assessing carbon storage and sequestration by Canada's urban forests using high resolution Earth observation data," *Urban Forestry Urban Greening*, vol. 13, no. 3, pp. 484–494, 2014.
[16] S. M. Raciti, L. R. Hutyra, and J. D. Newell, "Mapping carbon storage in urban trees with multi-source remote sensing data: Relationships between biomass, land use, and demographics in Boston neighborhoods," *Sci. Total Environ.*, vol. 500, pp. 72–83, 2014.
[17] A. M. Sousa, A. C. Gonçalves, P. Mesquita, and J. R. M. da Silva, "Biomass estimation with high resolution satellite images: A case study of Quercus rotundifolia," *ISPRS J. Photogramm. Remote Sens.*, vol. 101, pp. 69–79, 2015.
[18] S. C. Popescu, R. H. Wynne, and R. F. Nelson, "Measuring individual tree crown diameter with LiDAR and assessing its influence on estimating forest volume and biomass," *Can. Remote Sens.*, vol. 29, no. 5, pp. 564–577, 2003.
[19] Q. Xu, Z. Hou, M. Maltamo, and T. Tokola, "Calibration of area based diameter distribution with individual tree based diameter estimates using airborne laser scanning," *ISPRS J. Photogramm. Remote Sens.*, vol. 93, pp. 65–75, 2014.
[20] W.Y. Yan, A. Shaker, and N. El-Ashmawy, "Urban land cover classification using airborne LiDAR data: A review," *Remote Sens. Environ.*, vol. 158, pp. 295–310, 2015.
[21] C. Hopkinson, L. Chasmer, C. Gynan, C. Mahoney, and M. Sitar, "Multisensor and multispectral LiDAR characterization and classification of a forest environment," *Can. J. Remote Sens.*, vol. 42 pp. 501–520, Jun. 2016.
[22] *DMTI. Land Cover Region*, Geospatial Center at University of Waterloo, Waterloo, ON, USA, 2015, Accessed on: Jul. 2017.
[23] *First Base Solutions*. Google Earth, Town of Whitchurch-Stouffville, ON, Canada. 2016. [Online]. Available:http://www.earth.google.com. Accessed on: Feb. 26, 2016
[24] *Community of Stouffville Urban Design Guidelines*, Brook McIlroy, Inc., Toronto, ON, Canada, 2002.
[25] M. C. Lambert, C. H. Ung, and F. Raulier, "Canadian national tree aboveground biomass equations," *Can. J. Forest Res.*, vol. 35, no. 8, pp. 1996–2018, 2005.
[26] Q. Chen, D. Baldocchi, P. Gong, and M. Kelly, "Isolating individual trees in a savanna woodland using small footprint LiDAR data," *Photogramm. Eng. Remote Sens.*, vol. 72, no. 8, pp. 923–932, 2006.
[27] K. Zhao, S. Popescu, and R. Nelson, "Lidar remote sensing of forest biomass: A scale-invariant estimation approach using airborne lasers," *Remote Sens. Environ.*, vol. 113, no. 1, pp. 182–196, 2009.
[28] X. Yu, J. Hyyppä, H. Kaartinen, and M. Maltamo, "Automatic detection of harvested trees and determination of forest growth using airborne laser scanning," *Remote Sens. Environ.*, vol. 90, no. 4, pp. 451–462, 2004.
[29] H. Kaartinen *et al.*, "An international comparison of individual tree detection and extraction using airborne laser scanning," *Remote Sens.*, vol. 4, no. 4, pp. 950–974, 2012.
[30] E. Hadaś and J. Estornell, "Accuracy of tree geometric parameters depending on the LiDAR data density," *Eur. J. Remote Sens.*, vol. 49, pp. 73–92, 2016.
[31] M. Hauglin, J. Dibdiakova, T. Gobakken, and E. Næsset, "Estimating single-tree branch biomass of Norway spruce by airborne laser scanning," *ISPRS J. Photogramm. Remote Sens.*, vol. 79, pp. 147–156, 2013.
[32] S. C. Popescu, "Estimating biomass of individual pine trees using airborne LiDAR," *Biomass Bioenergy*, vol. 31, no. 9, pp. 646–655, 2007.

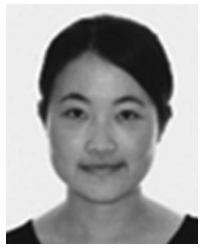

Xinqu Chen received the B.Sc. degree in environmental science from York University, Toronto, ON, Canada, in 2014, and the M.Sc. degree in geomatics from the University of Waterloo, Waterloo, ON, in 2016.

Her research interests include multispectral LiDAR data processing, land cover classification, forest inventory, and urban carbon storage estimation.

Chengming YE received the B.Sc. degree in surveying and mapping engineering from Taiyuan University of Technology, Taiyuan, China, in 2001, and the M.Sc. and Ph.D. degrees in geographic information science from Chengdu University of Technology, Chengdu, Sichuan, China, in 2007 and 2011, respectively.

He was a Visiting Scholar with the Department of Geography and Environmental Management, University of Waterloo, Waterloo, ON, Canada, during 2016–2017. He is currently an Associate Professor with the Key Laboratory of Earth Exploration and Information Technology of Ministry of Education, Chengdu University of Technology. His research interests include GIS, remote sensing, spatial modeling, and land cover classification.

Jonathan Li (M'00–SM'11) received the Ph.D. degree in geomatics engineering from the University of Cape Town, Cape Town, South Africa, in 2000.

He is currently a Professor with the Departments of Geography and Environmental Management and Systems Design Engineering, University of Waterloo, Waterloo, ON, Canada. He has coauthored more than 400 publications, including more than 170 refereed journal papers. His main research interests include LiDAR and SAR data processing, machine learning, and remote sensing applications.

Dr. Li is currently an Associate Editor of the IEEE JOURNAL OF SELECTED TOPICS IN APPLIED EARTH OBSERVATIONS AND REMOTE SENSING and the IEEE TRANSACTIONS ON INTELLIGENT TRANSPORTATION SYSTEMS.

Michael A. Chapman received the Ph.D. degree in photogrammetry from Laval University, Québec City, QC, Canada, in 1990.

He was a Professor of geomatics engineering with the University of Calgary, Canada, for 18 years. He is currently a Professor with the Department of Civil Engineering, Ryerson University, Toronto, ON, Canada. He has authored or coauthored more than 160 technical articles. His research interests include algorithms and processing methodologies for airborne sensors using global navigation satellite system/inertial measurement unit, geometric processing of digital imagery in industrial environments, terrestrial imaging systems for transportation infrastructure mapping, and algorithms and processing strategies for biometrology applications.